12-1988

Projectile Electron Capture and Loss Accompanying Target Ionization for Highly-Charged Oxygen Ions Colliding with Helium

Reynold N. Price
Western Michigan University

PROJECTILE ELECTRON CAPTURE AND LOSS ACCOMPANYING TARGET IONIZATION FOR HIGHLY-CHARGED OXYGEN IONS COLLIDING WITH HELIUM

by

Reynold N. Price

A Thesis
Submitted to the
Faculty of The Graduate College
in partial fulfillment of the
requirements for the
Degree of Master of Arts
Department of Physics

Western Michigan University
Kalamazoo, Michigan
December 1988

PROJECTILE ELECTRON CAPTURE AND LOSS ACCOMPANYING TARGET IONIZATION FOR HIGHLY-CHARGED OXYGEN IONS COLLIDING WITH HELIUM

Reynold N. Price, M.A.

Western Michigan University, 1988

Cross sections for electron capture and loss associated with target ionization are measured for highly charged O^{q+} (q=5,6,7,8+) ions colliding with helium at energies of 0.25 to 2.5 MeV/u. Experimentally, charge-changed projectile ions are detected in coincidence with specific target recoil-ion charge states. The fraction of transfer ionization (TI) relative to total electron capture is measured and compared to previous studies. The results show that TI is responsible for a significant percentage of the total single-electron-capture cross sections even at high velocities. Ratios of double- to single-target ionization are determined when simultaneous ionization of the projectile also occurs. The results show that double-ionization of the helium target is much more likely (about 4-5 times) to occur when the O^{q+} projectile ion is ionized than when it is not.

ACKNOWLEDGEMENTS

I would like to express my appreciation to the Department of Physics at Western Michigan University and the faculty members with whom I've been associated for the opportunity to further my studies. I also would like to specifically thank Dr. John A. Tanis for the effort he expended in guiding my thesis work, and Dr. Mark Clark for all his help and guidance.

My special thanks are for Juanita who has always been patient and has always supported me, and for Caleb and Micah who have always made me happy.

Reynold N. Price

7

13

3570 9

Order Number 1335709

Projectile electron capture and loss accompanying target ionization for highly-charged oxygen ions colliding with helium

Price, Reynold N., M.A.

Western Michigan University, 1988

U·M·I
300 N. Zeeb Rd.
Ann Arbor, MI 48106

TABLE OF CONTENTS

LIST OF TABLES

LIST OF FIGURES

CHAPTER I

INTRODUCTION

A variety of processes may occur when a fast projectile ion collides with a neutral target atom. Processes involving charge transfer, electron loss, and excitation are fundamental to the understanding of atomic interactions and have therefore been the subject of both theoretical and experimental studies (Betz, 1972; Janev and Hvelplund, 1981). Interest in understanding these processes also stems from their importance to other fields such as plasma physics (Drawin, 1980) and astrophysics (Steigman, 1975).

Single-charge transfer results when a projectile ion captures an electron from a target atom in a collision,

$$A^{q+} + B \longrightarrow A^{(q-1)+} + B^{+}, \qquad (1)$$

where the projectile ion and the target atom are represented by A and B, respectively, and the incident projectile ion charge state is given by q+. Single-electron loss results when the projectile ion loses an electron,

$$A^{q+} + B \longrightarrow A^{(q+1)+} + B + e^{-}. \qquad (2)$$

Multiple-electron charge-changing interactions may also occur and are generally described by

$$A^{q+} + B \longrightarrow A^{(q+/-n)+} + B^{i+} + (i+/-n)e^{-}. \qquad (3)$$

In this study, multiple-electron processes involving

target ionization associated with single charge-changing projectile events, i.e.

$$A^{q+} + B \longrightarrow A^{(q-1)+} + B^{i+} + (i-1)e^- \quad (i>1) \qquad (4)$$

and

$$A^{q+} + B \longrightarrow A^{(q+1)+} + B^{i+} + (i+1)e^- \quad (i>0) \qquad (5)$$

are investigated. The former process is referred to as transfer ionization (TI) while the latter we will call loss and ionization (LI).

Since the charge state of the resulting target recoiling ion is of concern in these processes, it must be identified along with the charge state of the projectile ion following the collision. Cross sections for charge-changed projectile ions associated with recoil ions in a particular charge state are measured using coincidence techniques.

When these coincidence measurements are made, the cross section for direct single capture, which is denoted by $\sigma^{01}_{q,q-1}$, can be distinguished from that for transfer ionization, denoted by $\sigma^{02}_{q,q-1}$. In this notation, the superscript gives the initial and final charge states of the target atom and the subscript refers to the initial and final charge states of the projectile ion. Similarly, for simultaneous projectile loss and target ionization, the cross sections are represented by $\sigma^{01}_{q,q+1}$ and $\sigma^{02}_{q,q+1}$.

In this work, highly charged oxygen (q=5,6,7,8+) colliding with a helium target over an energy range of

.25 to 2.5 MeV/u is studied. The purpose of this study is to investigate the importance of two- (and three-) electron processes involving projectile capture and loss accompanying target ionization, and to compare these cross sections to the corresponding one-electron cross sections. The results are also compared with the predictions of theory where possible.

CHAPTER II

EXPERIMENTAL PROCEDURE AND DATA ANALYSIS

The experiment was conducted at Western Michigan University in Kalamazoo, Michigan using the EN tandem Van de Graaff accelerator. A general schematic of the accelerator and beamline is shown in Figure 1. Highly charged oxygen ions (q=5-8+) were obtained by passing the accelerated ion through a carbon post-stripping foil. The beam was collimated by two apertures (area $\approx$ 1 mm^2) before entering the target region.

After interaction with the target gas, the beam was magnetically analyzed and the charge-changed components were detected using silicon surface barrier detectors. One detector was used to detect oxygen ions that had captured an electron, and the other detected ions that had lost an electron. The main beam (no charge change) was collected in a Faraday cup (suppressed at -300 volts) and the current measured with a Keithley electrometer.

The target region, shown in Figure 2, consisted of a differentially pumped gas cell 4.0 cm in length. The beam entered the area of interaction by passing through two apertures of diameters 0.080 and 0.120 inches and exited through two more apertures of diameters 0.120 inches. Two electrodes, held at +1000 and -1000 volts, extracted and

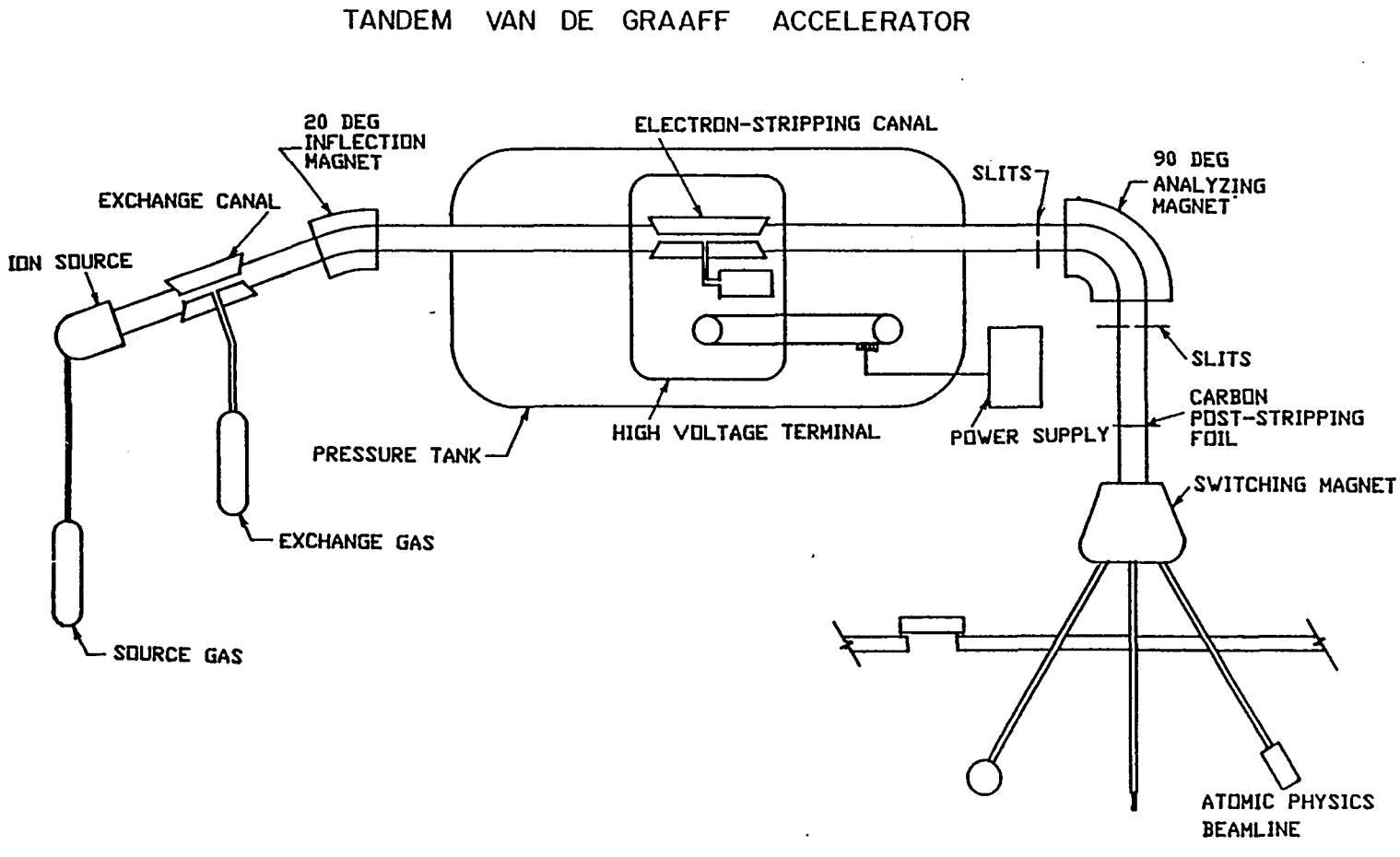

Figure 1. General Schematic of the WMU EN Tandem Van de Graaff Accelerator.

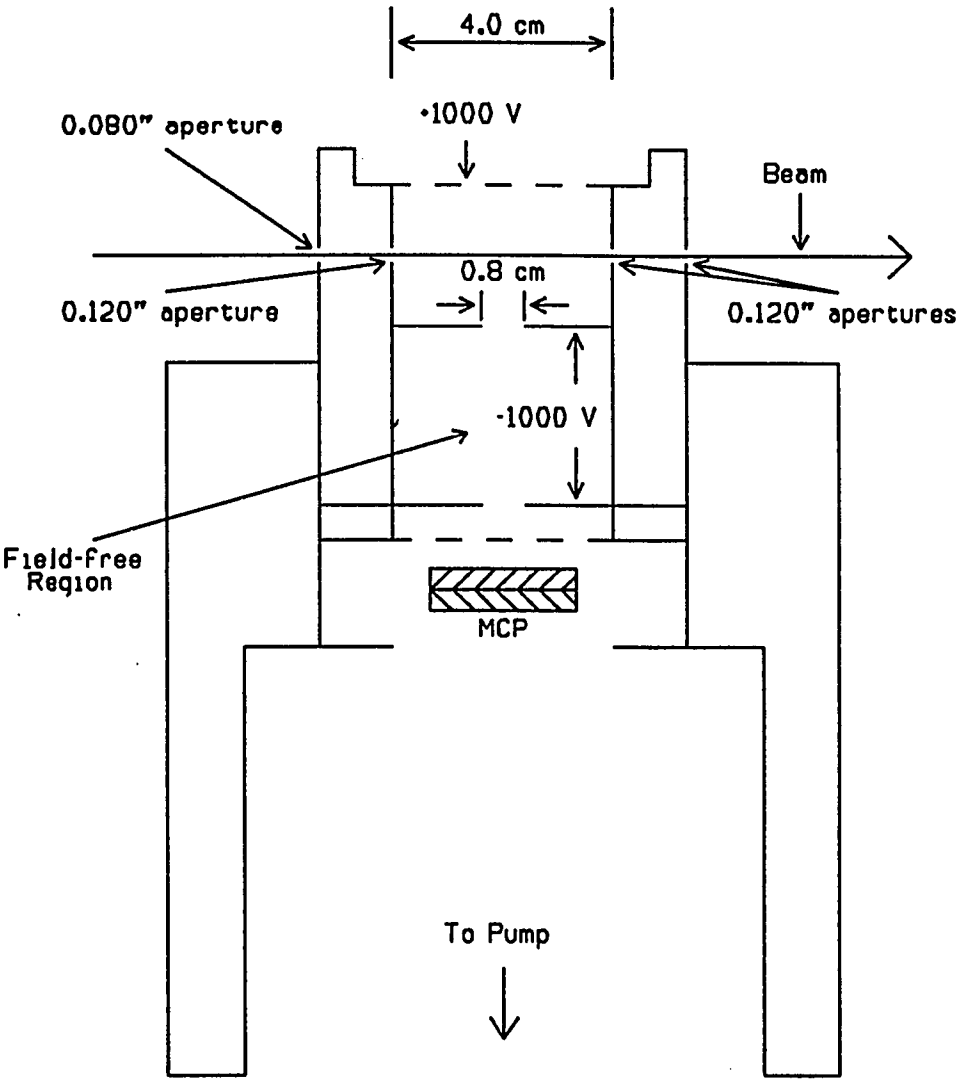

Figure 2. Schematic of the Target Region Consisting of a Differentially Pumped Gas Cell.

accelerated the helium recoil ions from the middle 0.8 cm of the interaction region. After drifting through a field-free region, the recoil ions passed through a repelling grid (to suppress electrons) and were detected with a negatively biased micro-channel plate (MCP).

Time-of-flight techniques were used to detect coincidences between oxygen ions capturing or losing an electron and the occurrence of singly- or doubly-charged helium recoil ions as shown in Figure 3. Signals from the micro-channel plate were passed through a fast preamplifier (FPA) and then routed to a timing filter amplifier (TFA) and a constant fraction discriminator (CFD). The constant fraction discriminator converted the analog signal to a logic signal which was used as a START for a time-to-amplitude converter (TAC).

Signals resulting from charge-changed oxygen ions striking the surface barrier detectors (SB) were also routed through pre-amplifiers and timing filter amplifiers. These signals, however, were delayed by about 750 ns (using long cables) before reaching the constant fraction discriminators. The output of the CFDs were then used as STOPs for the time-to-amplitude converters. The TACs output a signal whenever a START and a STOP were received within the full-scale time range selected on the TAC, and the amplitude of this signal (which depends on the time difference between the START and STOP signals) was used

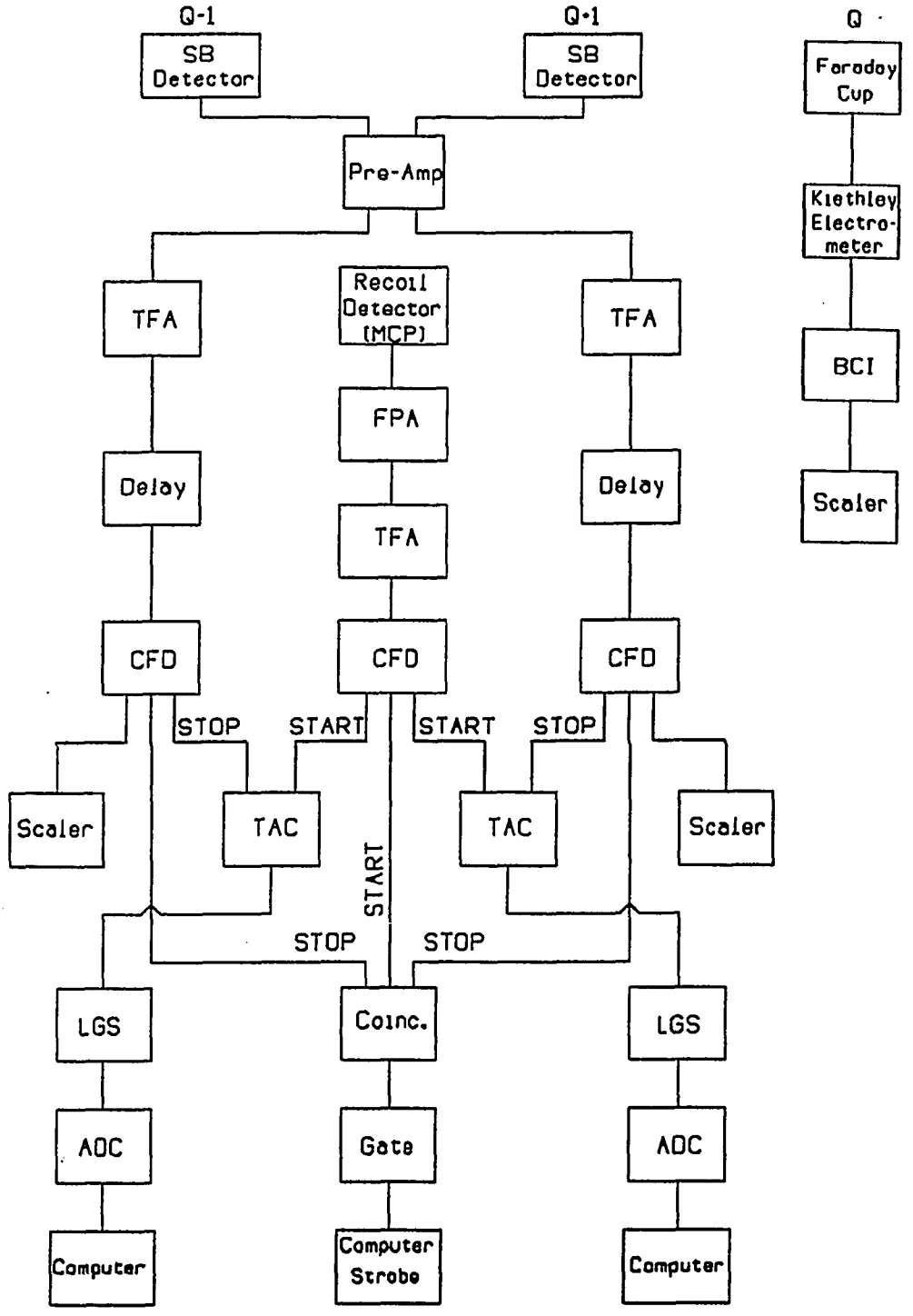

Figure 3. Electronic Configuration for Detecting Charge-Changed Projectile Ions in Coincidence With Target Recoil Ions.

to determine the charge state of the recoiling helium ion. The signals from the TACs were conditioned by the linear-gate-stretchers (LGS) prior to analysis by the analog-to-digital-converters.

A Keithley electrometer measured the main beam current which was typically on the order of a few picoamps. The incident particle yield was then obtained by integrating the current over the time required for the measurement with a beam current integrator (BCI).

Each run for a particular projectile ion energy and charge state was performed at different target gas cell pressures as measured by a capacitance manometer. Figures 4 and 5 are representative of the spectra resulting from a run at a given gas pressure. The spectrum for each pressure was analyzed to obtain fractional yields which were plotted as functions of gas pressure. Linearity of the plot indicated that single collision conditions prevailed within the target region (see Figure 6). Pressures less than or equal to 0.5×10^{-3} Torr were generally found to satisfy this condition.

A linear least-squares fit was applied to the appropriate region of the plots of measured fractions vs. gas pressure. The slopes of the resulting lines were used to obtain cross section values as described below.

The measured fraction (F) is defined as the ratio of the number of detected particles (N_x) to the total number

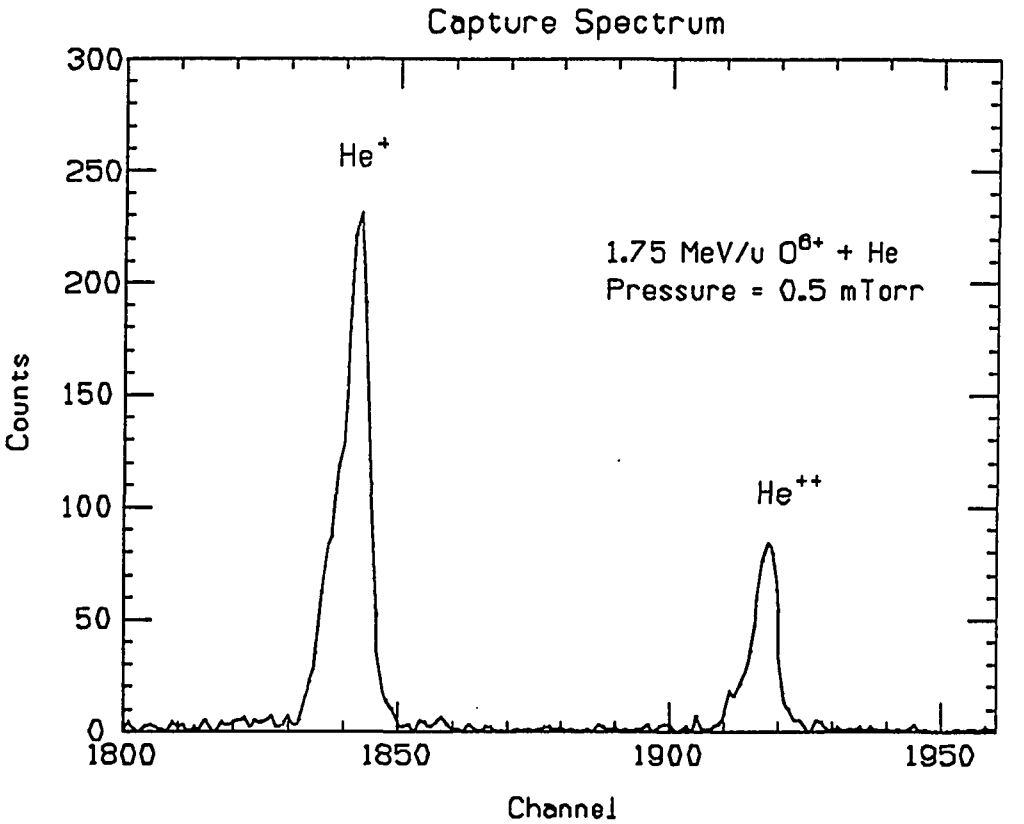

Figure 4. Typical Spectrum for Electron Capture by the Projectile Ion in Coincidence With Single and Double Ionization of the Target.

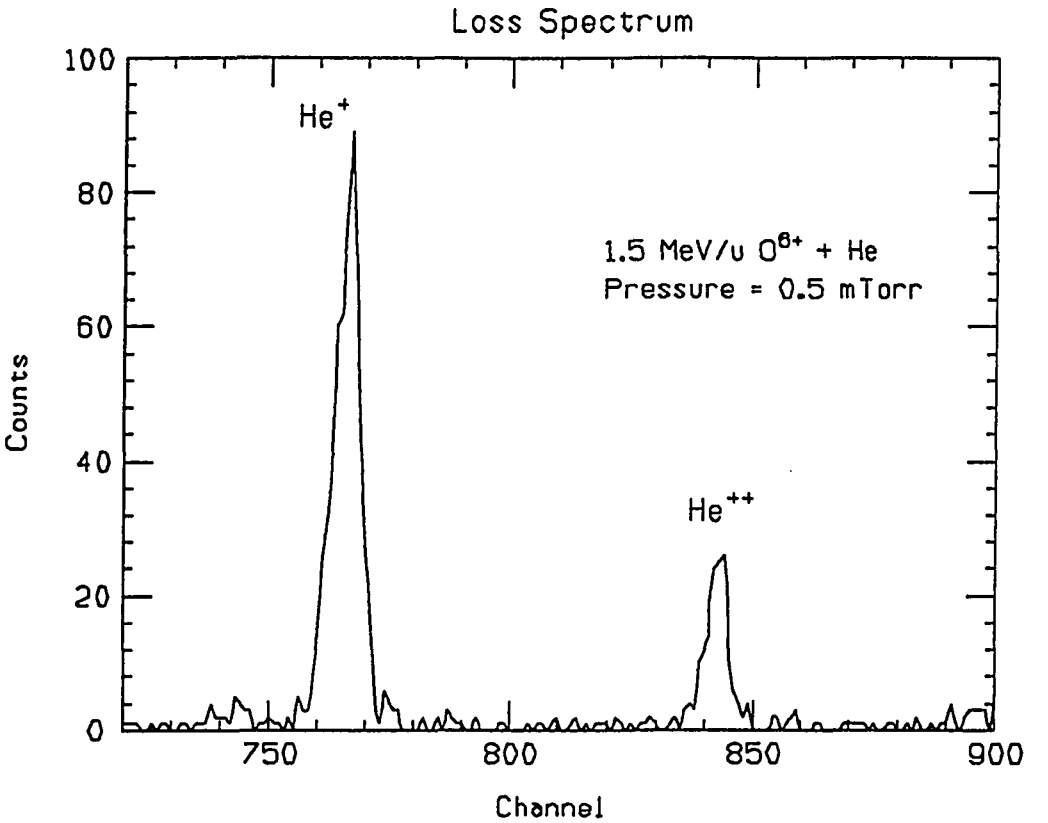

Figure 5. Typical Spectrum for Electron Loss From the Projectile Ion in Coincidence With Single and Double Ionization of the Target.

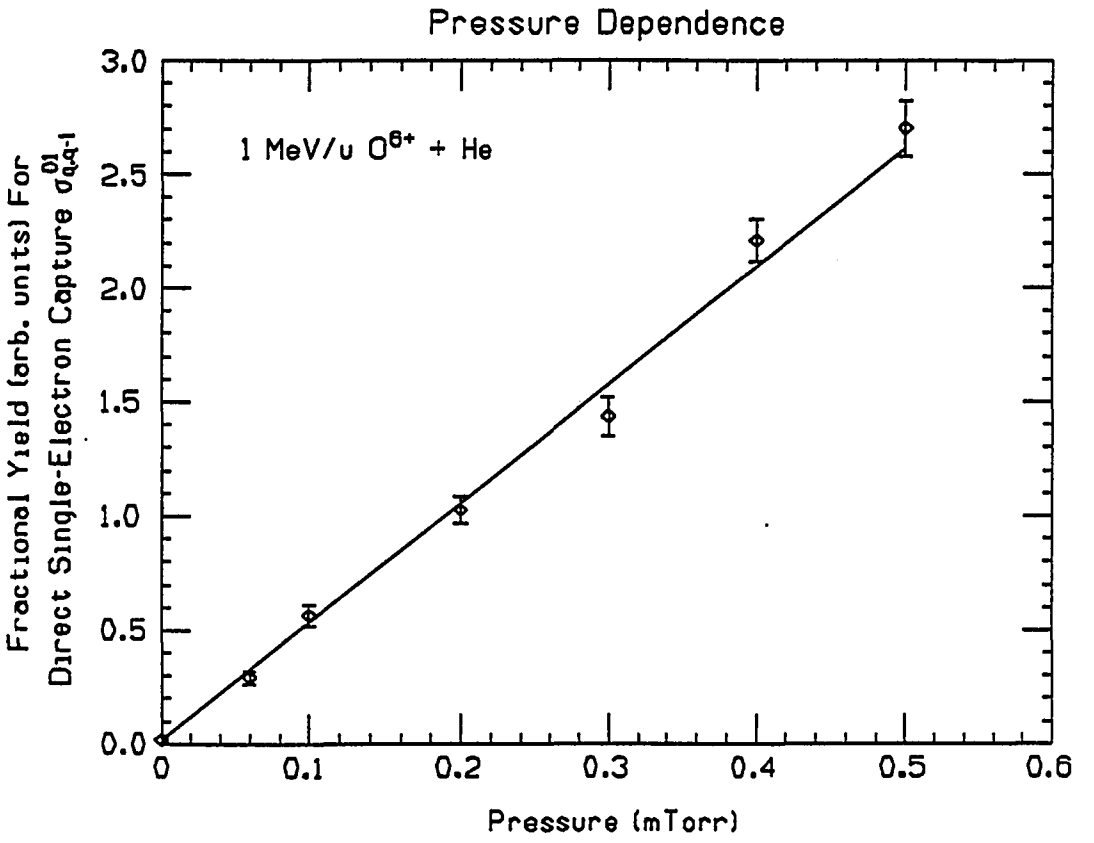

Figure 6. Typical Pressure Dependence Exhibiting Single-Collision Conditions.

of incident particles (I_o),

$$F = N_x/I_o. \tag{6}$$

The number of detected particles is given by

$$N_x = I_o\sigma T, \tag{7}$$

where σ is the cross section in units of cm^2/atom and T is the target thickness in units of atoms/cm^2. The target thickness is determined by

$$T = N_oPL, \tag{8}$$

where $N_o = 3.3 \times 10^{13}$ atoms/mTorr cm^3, P is the pressure in mTorr, and L is the length of the target cell in cm. Equation (6), used with equations (7) and (8), then leads to

$$F = \sigma N_oPL, \tag{9}$$

$$\Delta F = \sigma N_oL\Delta P, \tag{10}$$

and

$$\sigma = \Delta F/\Delta PN_oL, \tag{11}$$

where $\Delta F/\Delta P$ represents the slope of the plot of yield vs. gas pressure.

To obtain absolute concidence cross sections, it is noted that the sum of the cross sections for capture in coincidence with singly- and doubly-charged helium recoil ions must necessarily be equal to the total cross section $\sigma_{q,q-1}$ for single-electron capture, i.e.,

$$\sigma_{q,q-1} = \sigma^{01}_{q,q-1} + \sigma^{02}_{q,q-1}. \tag{12}$$

Due to beam integration difficulties, accurate total capture cross sections were not obtained, so the present

data were normalized to previously published results (MacDonald and Martin, 1971; Hvelplund, Haugen, and Knudsen, 1981; Dillingham, Macdonald, and Richard, 1981). These earlier data are adequately described by the empirical scaling curve of Schlachter, et al. (1987) which was then used to provide the total single-capture cross section for each projectile energy and charge state. These cross sections, along with the measured ratio of slopes ($\Delta F/\Delta P$) for singly- and doubly- charged recoil ions obtained from the pressure dependence curves (see Figure 6), then give the cross sections for capture in coincidence with helium recoil ions according to the relations

$$\sigma^{01}_{q,q-1} = \frac{(\Delta F/\Delta P)_+}{(\Delta F/\Delta P)_+ + (\Delta F/\Delta P)_{++}} \sigma_{q,q-1} \qquad (13)$$

and

$$\sigma^{02}_{q,q-1} = \frac{(\Delta F/\Delta P)_{++}}{(\Delta F/\Delta P)_+ + (\Delta F/\Delta P)_{++}} \sigma_{q,q-1}. \qquad (14)$$

In these equations the slopes for singly- and doubly-charged recoil ions are represented by $(\Delta F/\Delta P)_+$ and $(\Delta F/\Delta P)_{++}$, respectively.

To calculate the cross sections for target ionization associated with projectile electron loss, an effective efficiency for recoil-ion detection was determined from the ratio of the sum of the coincidence slopes for capture to the total capture cross sections predicted by

the empirical scaling rule of Schlachter, et al. (1987), i.e.,

$$\varepsilon = [(\Delta F/\Delta P)_{+} + (\Delta F/\Delta P)_{++}](1/N_{o}L)/\sigma_{q,q-1} \qquad (15)$$

This efficiency ε was then used in conjunction with equation (11) to determine the cross sections

$$\sigma^{01}_{q,q+1} = (\Delta F/\Delta P)_{+}(1/N_{o}L) \times 1/\varepsilon, \qquad (16)$$

and

$$\sigma^{02}_{q,q+1} = (\Delta F/\Delta P)_{++}(1/N_{o}L) \times 1/\varepsilon, \qquad (17)$$

for projectile loss in coincidence with singly- and doubly-charged recoil ions.

Sources of error in the cross sections obtained include counting statistics (about 5%), beam current normalization (5%), determination of gas pressure (5%), calibration of the Keithley electrometer and beam current integrator (<5%), and length of the gas cell (<10%), in addition to the error associated with fitting a line to the yield vs. pressure data (typically 5-15%). The fitting errors were derived from the weighted standard deviations of the slopes (see Figure 6), and include the uncertainties associated with the counting statistics and beam current integration. The empirical scaling rule of Schlachter, et al. (1987) was assumed to have an uncertainty of approximately 30%. Absolute errors were then derived by combining all of these uncertainties in quadrature.

An additional error may be associated with the con-

tribution to target ionization produced by projectiles which capture or lose an electron in the residual gas in the beam line prior to reaching the target. These projectiles can ionize the target gas without further charge change and be detected as coincidence events. The cross sections for such events are larger than those for projectiles which produce target ionization and undergo charge change in the target region. It is not possible at present to estimate the relative magnitude of this uncertainty.

CHAPTER III

CAPTURE-COINCIDENCE MEASUREMENTS

Electron capture in collisions between ions and atoms has been studied for many years (see Betz, 1972 and Hvelplund, Haugen, and Knudsen, 1981). However, the process is complicated by the fact that additional electrons may be lost from the target, a process referred to as transfer ionization (TI). No differentiation was made in most of these earlier studies between simple charge transfer and transfer ionization (equations (1) and (4)).

Several different mechanisms can contribute to the transfer-ionization process. For example, in very slow collisions (< 1eV/u) Niehaus (1980) has shown that TI can result from autoionization of the quasimolecule formed during the collision. At higher velocities (≈ 100 eV/u) Cocke, DuBois, Grey, Justiniano, and Can (1981) have attributed TI to double capture by the projectile followed by autoionization. At velocities near 100 keV/u, Andersen, Frost, Hvelplund, Knudsen, and Datz (1984) have obtained evidence that TI is due to the correlated transfer of two electrons to the projectile ion followed by the subsequent loss of one of these electrons to the continuum. At higher energies (> 1 MeV/u), where the electrons can be treated independently, TI is expected to be

due mainly to single electron capture plus direct impact ionization of the target.

In most of the measurements reported to date, which have been done primarily for velocities < 1 MeV/u, TI has been found to account for less than 30% of all the events leading to capture of a single electron. However, recent measurements (Datz, et al., 1987) for I^{q+} and U^{q+} show TI fractions of about 70%. Olson, Wetmore, and McKenzie (1986) have calculated for 1 MeV/u projectiles of charge state q > 10 that TI may be responsible for up to 80% of all the total single-electron capture events occuring in a collision.

In order to assess the importance of the two-electron TI process relative to total single capture in the 1 MeV/u energy regime, cross sections have been determined for single-electron capture in coincidence with single-electron loss from the target, $\sigma^{01}_{q,q-1}$ (direct capture), and with double-electron loss from the target, $\sigma^{02}_{q,q-1}$ (transfer ionization). These cross sections are listed with their associated absolute errors in Table 1 and plotted in Figures 7 and 8. The figures show cross sections which decrease with energy from about 1×10^{-16} cm^2 to less than 1×10^{-20} cm^2 and increase slightly with charge state. These cross sections can be used to define the fraction

Table 1

Cross Sections for Electron Capture in Coincidence With Single and Double Ionization of the Helium Target Atom

q	E (MeV/u)	$\sigma^{01}_{q,q-1}$ (cm^2) ($\times 10^{-19}$)			$\sigma^{02}_{q,q-1}$ (cm^2) ($\times 10^{-19}$)		
5	0.50	90	+/-	30	79	+/-	24
5	0.75	18	+/-	5	14	+/-	4
5	1.00	5.6	+/-	1.7	4.2	+/-	1.3
5	1.50	1.2	+/-	0.4	0.58	+/-	0.17
6	0.25	730	+/-	220	780	+/-	230
6	0.50	130	+/-	40	130	+/-	40
6	0.75	29	+/-	9	25	+/-	7
6	1.00	9.6	+/-	2.9	6.6	+/-	2.0
6	1.25	4.1	+/-	1.2	2.2	+/-	0.7
6	1.38	2.9	+/-	0.9	1.4	+/-	0.4
6	1.50	2.1	+/-	0.6	0.91	+/-	0.27
6	1.63	1.6	+/-	0.5	0.55	+/-	0.17
6	1.75	1.2	+/-	0.3	0.41	+/-	0.12
6	1.88	0.94	+/-	0.28	0.23	+/-	0.07
6	2.07	0.65	+/-	0.20	0.13	+/-	0.04
6	2.25	0.44	+/-	0.13	0.10	+/-	0.03
6	2.50	0.28	+/-	0.09	0.068	+/-	0.020
7	0.50	170	+/-	50	210	+/-	60
7	0.75	39	+/-	12	43	+/-	13
7	1.00	14	+/-	4	11	+/-	3
7	1.25	6.1	+/-	1.8	3.7	+/-	1.1
7	1.38	4.5	+/-	1.4	2.0	+/-	0.6
7	1.50	3.3	+/-	1.0	1.3	+/-	0.4
7	1.63	2.5	+/-	0.7	0.79	+/-	0.24
7	1.75	1.8	+/-	0.5	0.58	+/-	0.17
7	1.88	1.4	+/-	0.4	0.43	+/-	0.13
7	2.07	1.0	+/-	0.3	0.22	+/-	0.07
7	2.25	0.73	+/-	0.22	0.11	+/-	0.03
7	2.50	0.46	+/-	0.14	0.082	+/-	0.025
8	0.50	240	+/-	70	280	+/-	80
8	0.75	57	+/-	17	62	+/-	19
8	1.00	19	+/-	6	17	+/-	5
8	1.50	4.5	+/-	1.4	17	+/-	0.6

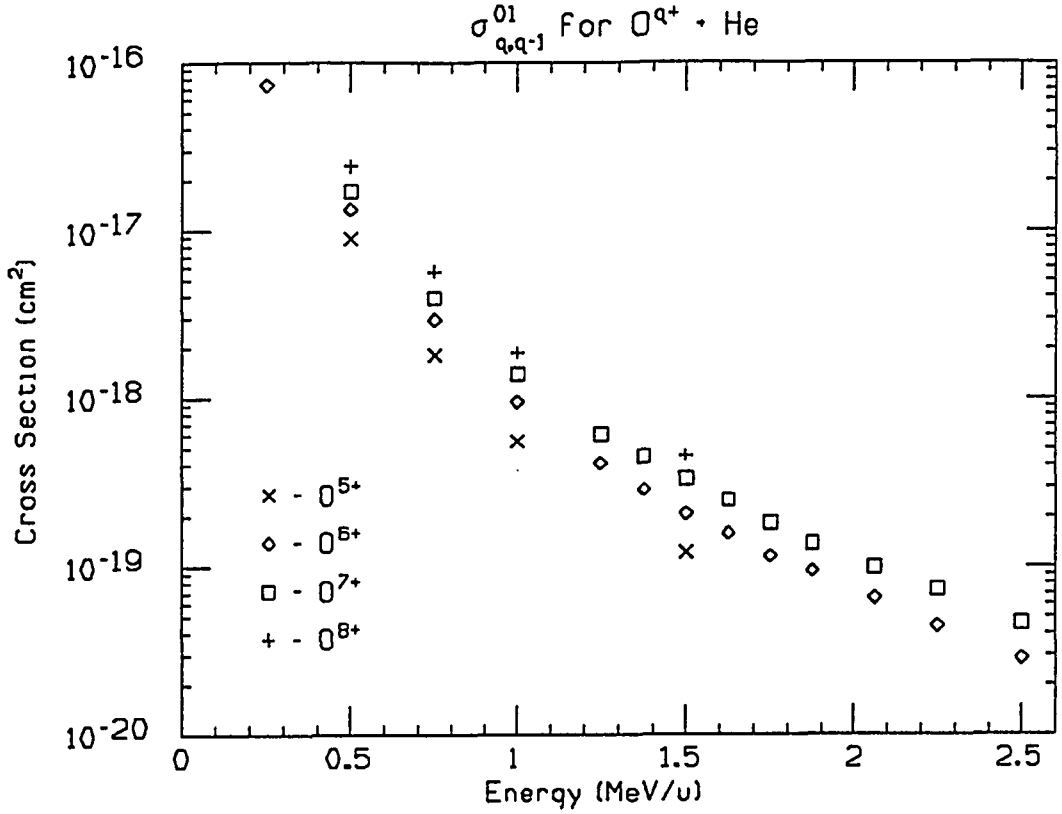

Figure 7. Cross Sections for Projectile Single-Electron Capture in Coincidence With Single Ionization of the Target Atom.

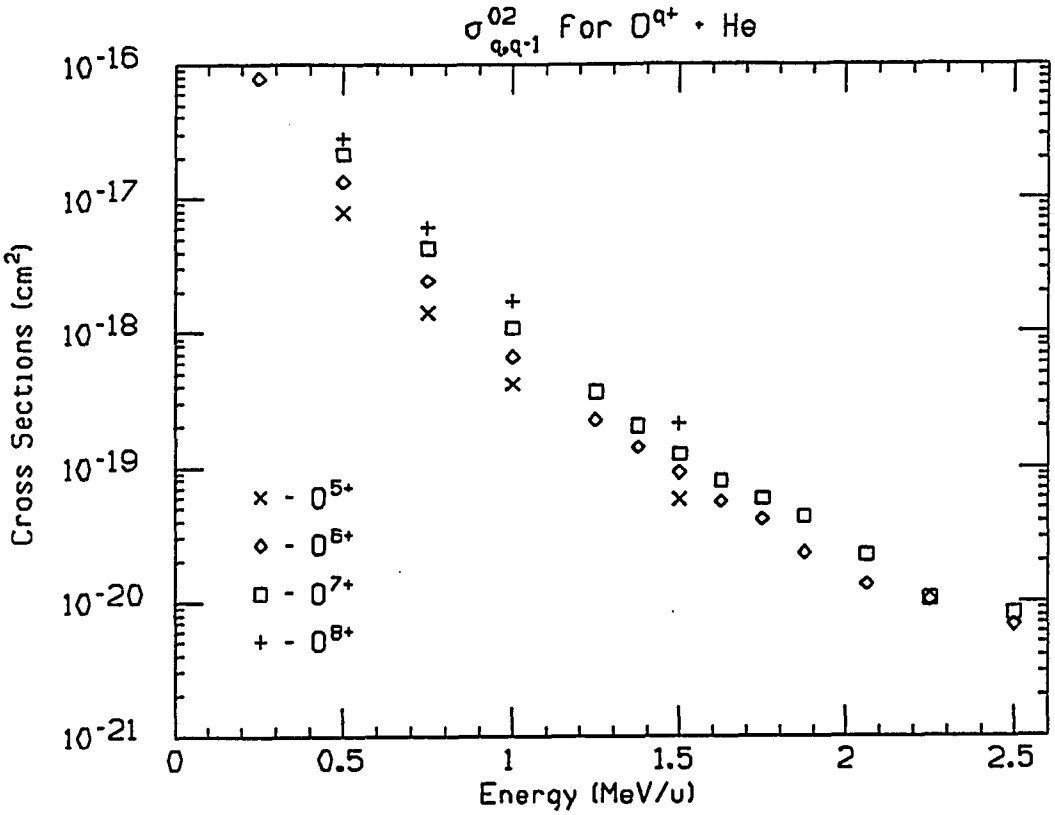

Figure 8. Cross Sections for Projectile Single-Electron Capture in Coincidence With Double Ionization of the Target Atom.

$$f = \frac{\sigma^{02}_{q,q-1}}{\sigma^{01}_{q,q-1} + \sigma^{02}_{q,q-1}}, \qquad (18)$$

which is the ratio of the transfer ionization cross section to the total cross section for single-electron capture. The fractions for the present measurements are tabulated in Table 2 and shown in Figure 9. It is seen from the figure that f decreases with energy and in general, increases slightly with charge state. Over the present

Table 2

Fraction of Transfer Ionization Relative to Total Single Capture

q	E(MeV/u)	f	q	E(MeV/u)	f
5	0.50	0.47 +/- 0.01	7	0.50	0.55 +/- 0.01
5	0.75	0.44 +/- 0.01	7	0.75	0.52 +/- 0.01
5	1.00	0.43 +/- 0.02	7	1.00	0.44 +/- 0.02
5	1.50	0.32 +/- 0.06	7	1.25	0.37 +/- 0.02
			7	1.38	0.31 +/- 0.02
6	0.25	0.52 +/- 0.01	7	1.50	0.27 +/- 0.03
6	0.50	0.50 +/- 0.01	7	1.63	0.24 +/- 0.02
6	0.75	0.46 +/- 0.01	7	1.75	0.24 +/- 0.02
6	1.00	0.41 +/- 0.01	7	1.88	0.24 +/- 0.03
6	1.25	0.35 +/- 0.03	7	2.07	0.18 +/- 0.04
6	1.38	0.33 +/- 0.02	7	2.25	0.13 +/- 0.08
6	1.50	0.31 +/- 0.04	7	2.50	0.15 +/- 0.05
6	1.63	0.26 +/- 0.03			
6	1.75	0.26 +/- 0.04	8	0.50	0.54 +/- 0.02
6	1.88	0.20 +/- 0.04	8	0.75	0.52 +/- 0.02
6	2.07	0.17 +/- 0.04	8	1.00	0.48 +/- 0.01
6	2.25	0.19 +/- 0.07	8	1.50	0.32 +/- 0.02
6	2.50	0.19 +/- 0.05			

range of energy and charge states, f varies from a high of about 55% for O^{7+} at 0.5 MeV/u to a low of approxi-

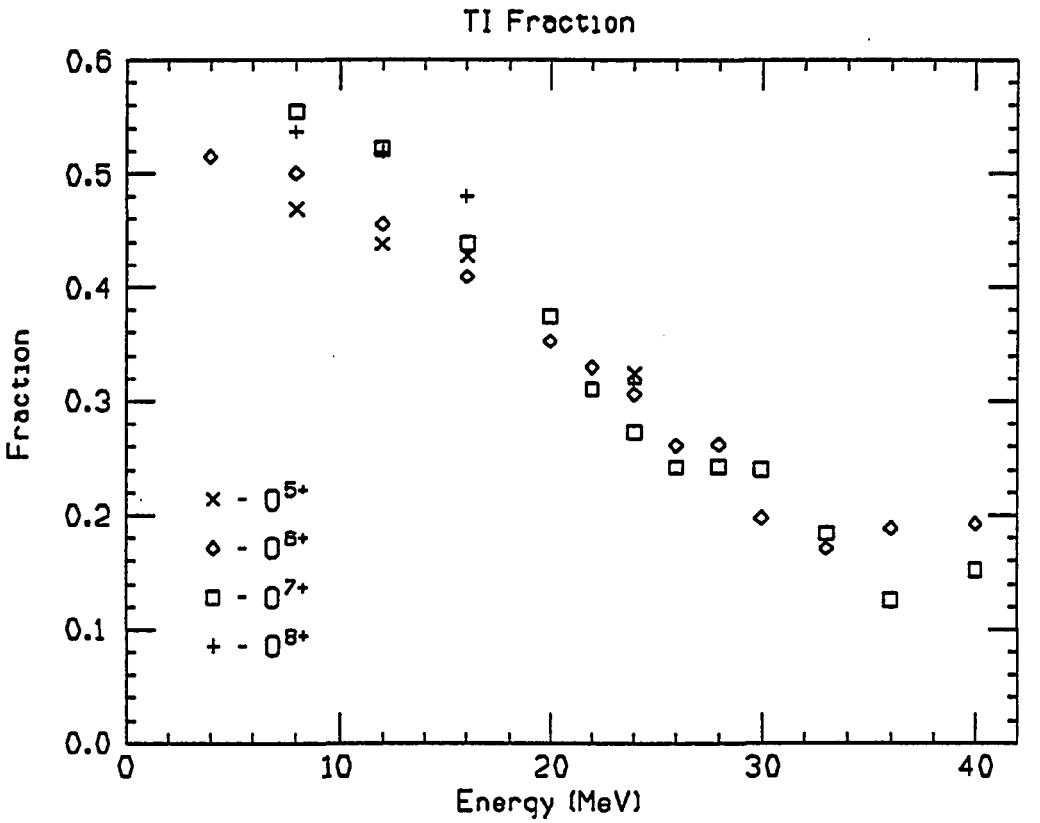

Figure 9. Ratio of Transfer Ionization Cross Sections to the Total Single-Electron-Capture Cross Section.

mately 15% for O^{7+} at 2.25 MeV/u.

The present data can be compared with previously reported measurements in order to investigate the behavior of TI over larger ranges of E and q. To take into account the energy and charge-state dependence of f for the various sets of available data, f is plotted as a function of the scaled energy $E/q^{0.5}$ and shown in Figure 10. In addition to the present values of f for O^{q+} ions with q = 5 to 8 and E = 250 to 2500 keV/u, the values of Shah and Gilbody (1985) for H^+, He^{2+}, and Li^{3+} ions with energies E = 30 to 500 keV/u are displayed, as well as the measurements by DuBois (1986) for He^{2+} at lower energies. Results are also available for Au^{q+} ions with q = 5 to 20 at 101.5 keV/u from studies by Damsgaard, Haugen, Hvelplund, and Knudsen (1983). Also included are measurements by Datz, et al. (1987) for I^{q+} with q = 5 to 16 at 100 and 250 keV/u and for U^{q+} with q = 17 to 30 at 250, 500, and 1000 keV/u. A single point, derived from results of Stockli, et al. (1986) for 3700 keV/u Ar^{17+} ions is also plotted.

These data suggest the existence of a peak in f for $E/q^{0.5} \approx 100$ keV/u. Such a maximum may indicate a transition from a region of lower energies where double capture followed by autoionization is the dominant mechanism for TI to a region of higher energies where single capture plus impact ionization dominates. Notably, the

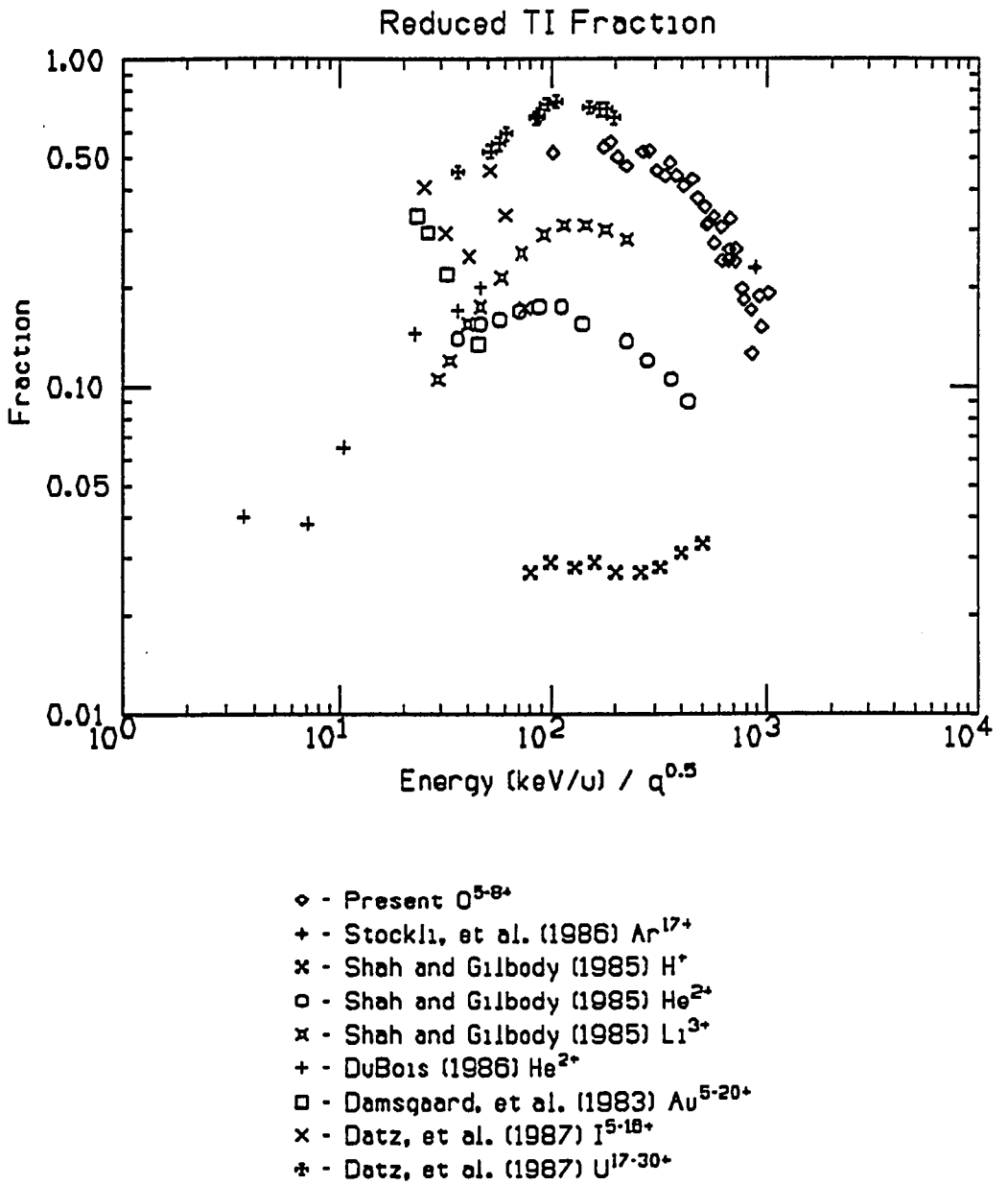

Figure 10. TI Fraction as a Function of $E(keV/u)/q^{0.5}$.

I^{q+} and Au^{q+} data deviate from the trend observed for the other measurements displayed in Figure 10.

Using the above mentioned measurements for H^+, He^{2+}, and Li^{3+}, McGuire, Salzborn, and Muller (1987), have previously noted the existence of a maximum in f. This maximum can be explained qualitatively in terms of classical arguments from which the most efficient projectile energy for ionizing the helium target atom is predicted to be when the projectile velocity matches the velocity of the bound target electron (see Betz, 1972). Since the binding energy of helium is about 25 eV, this would predict a maximum ionization probability for a velocity of about 50 keV/u, in rough agreement with the data of Figure 10. Experimentally, the ionization cross section for helium has been found to be at its maximum value for $E\ (keV/u)/q^{0.65} \approx 100$ (Phaneuf, Janev, and Pindzola, 1987), which is also similar to the results shown in Figure 10.

At energies greater than 100 keV/u, McGuire, et al. (1987) find that the TI fraction varies with a $(Z/v)^2$ scaling and they predict that this fraction should asymptotically approach a limiting value. Qualitatively, these authors argue that since the electron leaves the target atom quickly in a high speed collision, it might be expected that this limiting fraction will be the same as for photoionization where the electron similarly leaves the target very quickly and the other electron is then

ionized via a final-state rearrangement mechanism. It is suggested that this limiting value for heavy ions should then be the same as that found for p + He collisions at high velocity, i.e., $f \approx 0.03$.

Over the range of energies of the present measurements (250 - 2500 keV/u) the data approximately follow the suggested $(Z/v)^2$ scaling of McGuire, Salzborn, and Muller (1987). However, the data do not appear to approach a limiting value at the highest energies investigated. It is possible that at energies above this range the TI fractions may still approach the asymptotic value derived from photon data.

From the present data, it can be concluded that at high velocities the TI process is responsible for a significant percentage of the total single-electron-capture cross sections. First-order theories (Knudsen, Haugen, and Hvelplund, 1981; Schlachter, et al., 1983) of single-electron-capture have not always included such additional ionization mechanisms, and experimental measurements have not always distinguished between direct capture and TI. The failure to allow for the possibility of transfer ionization may therefore lead to large discrepancies between the predictions of theory and experimental results.

CHAPTER IV

LOSS-COINCIDENCE MEASUREMENTS

Measurements have previously been reported in the published literature for simultaneous ionization of the projectile ion and the target atom in a fast collision (Pedersen and Larsen, 1979; DuBois and Manson, 1986). However, these measurements have generally been for light projectile ions (H^+, He^+, and He^{2+}) incident upon helium and have concentrated on comparisons of projectile ionization data with theoretical calculations such as the plane-wave Born-approximation (Choi, Merzbacher, and Khandelwal, 1974). The present measurements are for a heavier projectile ion (oxygen 5-7+) incident on helium, in which cross sections for projectile ionization in coincidence with single and double target ionization are obtained.

Cross sections for loss of an electron from the projectile ion in coincidence with single ionization of the helium target $\sigma^{01}_{q,q+1}$ are shown in Figure 11 as a function of the energy of the incident oxygen ion. Cross sections $\sigma^{02}_{q,q+1}$ are displayed in Figure 12 and the values of both $\sigma^{01}_{q,q+1}$ and $\sigma^{02}_{q,q+1}$ are listed in Table 3 along with the absolute errors associated with these measurements.

It is noted that for an O^{7+} projectile, $\sigma^{01}_{q,q+1}$ and

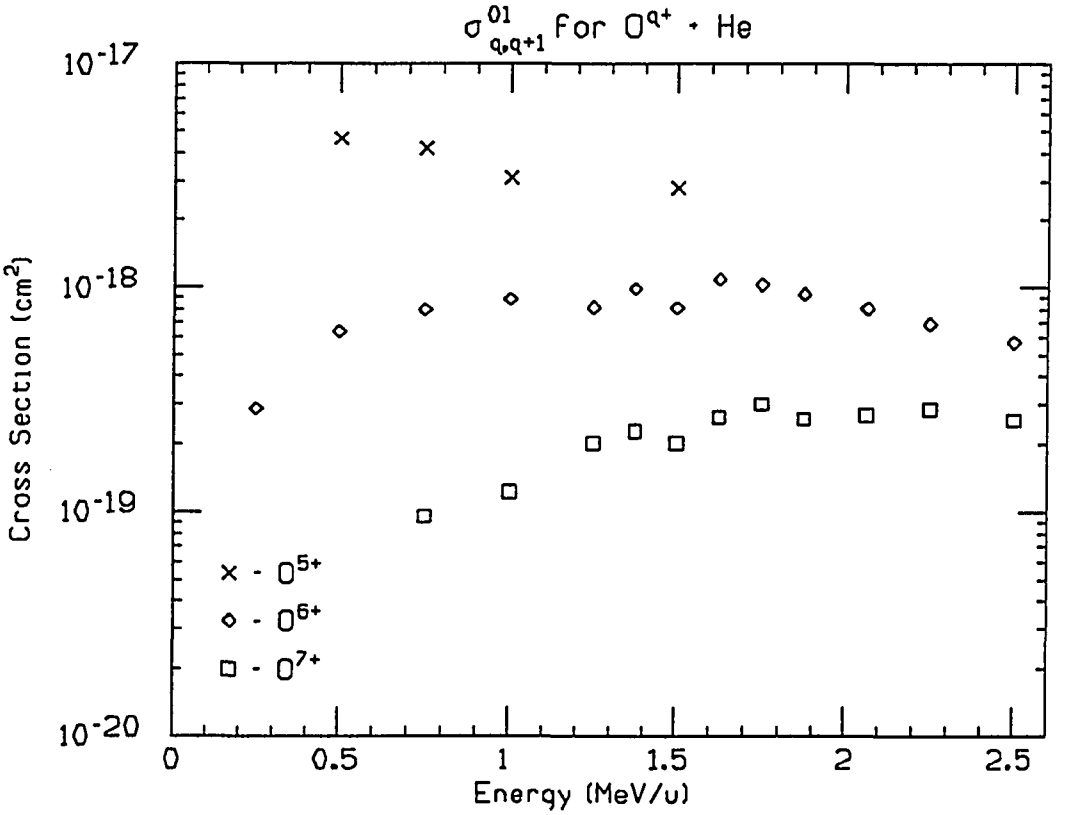

Figure 11. Cross Sections for Projectile Electron Loss in Coincidence With Single Ionization of the Target Atom.

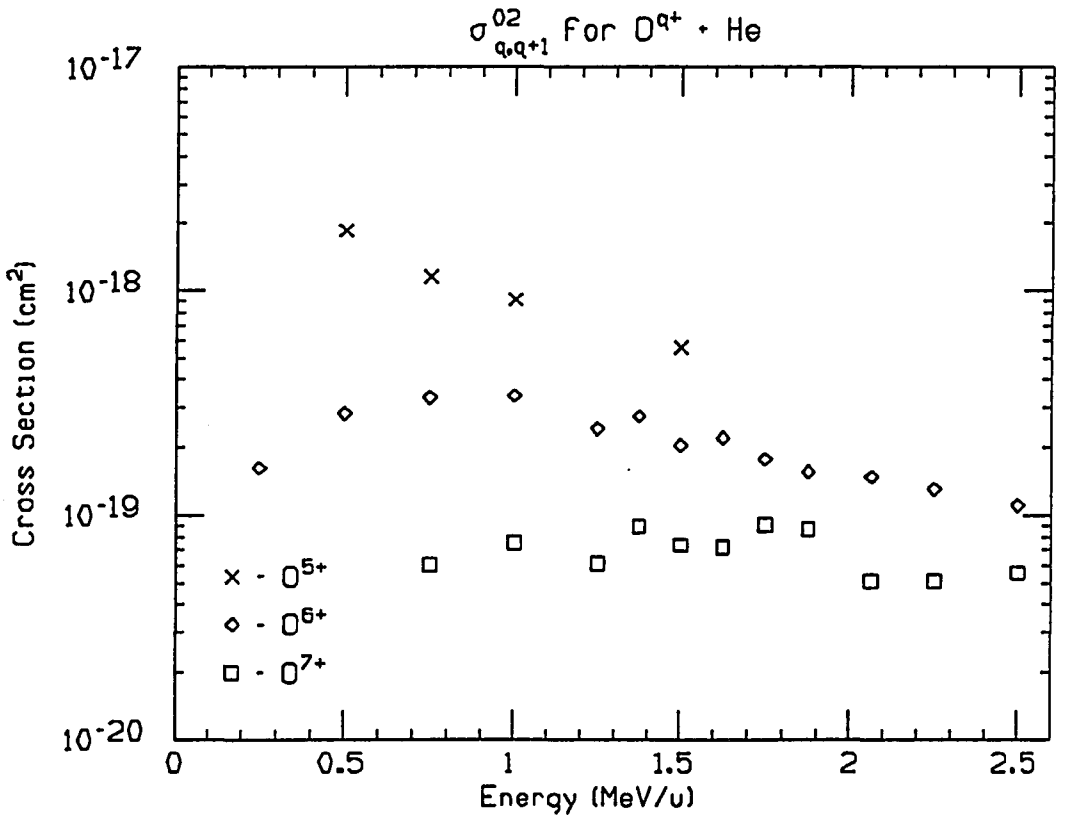

Figure 12. Cross Sections for Projectile Electron Loss in Coincidence With Double Ionization of the Target Atom.

Table 3

Cross Sections for Projectile Electron Loss in Coincidence With Single and Double Ionization of the Helium Target

q	E (MeV/u)	$\sigma^{01}_{q,q+1}$ (cm^2) ($\times 10^{-19}$)		$\sigma^{02}_{q,q+1}$ (cm^2) ($\times 10^{-19}$)	
5	0.50	46	+/- 14	18	+/- 5
5	0.75	42	+/- 13	10	+/- 3
5	1.00	31	+/- 9	9.2	+/- 2.8
5	1.50	27	+/- 8	5.6	+/- 1.7
6	0.25	2.9	+/- 0.9	1.6	+/- 0.5
6	0.50	6.3	+/- 1.9	2.8	+/- 0.9
6	0.75	8.0	+/- 2.4	3.3	+/- 1.0
6	1.00	8.9	+/- 2.7	3.4	+/- 1.0
6	1.25	8.1	+/- 2.4	2.4	+/- 0.7
6	1.38	9.9	+/- 3.0	2.8	+/- 0.8
6	1.50	8.1	+/- 2.4	2.1	+/- 0.6
6	1.63	11	+/- 3	2.2	+/- 0.7
6	1.75	10	+/- 3	1.8	+/- 0.5
6	1.88	9.3	+/- 2.8	1.6	+/- 0.5
6	2.07	8.1	+/- 2.4	1.5	+/- 0.4
6	2.25	6.9	+/- 2.1	1.3	+/- 0.4
6	2.50	5.7	+/- 1.7	1.1	+/- 0.3
7	0.75	0.95	+/- 0.29	0.60	+/- 0.18
7	1.00	1.2	+/- 0.4	0.76	+/- 0.23
7	1.25	2.0	+/- 0.6	0.61	+/- 0.18
7	1.38	2.3	+/- 0.7	0.90	+/- 0.27
7	1.50	2.0	+/- 0.6	0.74	+/- 0.22
7	1.63	2.6	+/- 0.8	0.72	+/- 0.22
7	1.75	3.0	+/- 0.9	0.90	+/- 0.27
7	1.88	2.6	+/- 0.8	0.86	+/- 0.26
7	2.07	2.7	+/- 0.8	0.51	+/- 0.15
7	2.25	2.9	+/- 0.9	0.51	+/- 0.15
7	2.50	2.6	+/- 0.8	0.55	+/- 0.17

$\sigma^{02}_{q,q+1}$ increase with energy until a maximum is reached at approximately 1.5 MeV/u. The cross section is then nearly constant with increasing energy possibly showing a slight decreasing trend. Qualitatively, such a pattern is expected.

Classical theory (see Betz, 1972) and the Bohr model predict that the removal of an electron from the target atom is most probable when the incident projectile approaches at the same velocity as the electron orbits the atom. The corresponding energy of the projectile ion is then given by the relation

$$E_{ion} = E_e (m_{ion}/m_e), \tag{19}$$

where

$$E_{ion} = 1/2\ m_{ion} v^2 \tag{20}$$

and

$$E_e = 1/2\ m_e v^2. \tag{21}$$

Equation (19) results because E_e is the binding energy of the electron in a circular orbit and can be determined (for a one-electron Bohr atom) in units of eV from

$$E_e = 13.6\ Z^2/n^2, \tag{22}$$

where Z is the atomic number of the target atom and n is the level of excitation of the electron.

Equations (19) and (22) predict that an O^{7+} projectile ion should have an energy of about 1.6 MeV/u to most effectively overcome the binding energy of the final K-electron. Figures 11 and 12 indicate that the maximum in

$\sigma^{01}_{q,q+1}$ and $\sigma^{02}_{q,q+1}$ occurs near this value in good quantitative agreement with the prediction.

For the case of O^{6+} projectile ions, the same trend is expected in the data. The maximum cross section should occur at a slightly lower energy though, since one K-electron screens the other from the oxygen nucleus, resulting in a slightly lower binding energy. This lower energy maximum for $\sigma^{01}_{q,q+1}$ and $\sigma^{02}_{q,q+1}$ is observed for O^{6+} in Figures 11 and 12.

When a third electron (i.e., a 2s electron) is present in the oxygen ion, the binding energy for that electron is less than for the higher charge states. The projectile energy corresponding to a maximum in $\sigma^{01}_{q,q+1}$ and $\sigma^{02}_{q,q+1}$ for O^{5+} is then predicted by equations (19) and (22) to be about .4 MeV/u, which occurs below the range of the present data. Figures 11 and 12 therefore show only the decrease of $\sigma^{01}_{q,q+1}$ and $\sigma^{02}_{q,q+1}$ with increasing energy for incident O^{5+} ions.

The same trends are noted for $\sigma^{02}_{q,q+1}$ as for $\sigma^{01}_{q,q+1}$ for all three charge states of the projectile ion. This indicates that when both the target atom and the projectile are ionized, the energy dependence is dominated by the ionization of the incident oxygen, even though ionization of the He target is much more likely. This is because ionization of the oxygen must occur in close collisions where the small impact parameters give rise to a high

probability for He ionization.

Of relevance to the present data is the work of DuBois and Manson (1986). These authors find that simultaneous ionization of both collision partners in He^+ + He occurs a large percentage of the time. From a comparison of their results with theoretical calculations, it is concluded that there is a correlation between the helium projectile electron and the helium target electrons in the ionization process. Currently, however, there is no way to determine whether such a correlation exists in the present data for oxygen colliding with helium.

The fact that $\sigma^{02}_{q,q+1}$ is generally less than $\sigma^{01}_{q,q+1}$ for any given energy reflects the lower probabilty of removing both electrons from the helium atom in these close (i.e., small impact parameter) collisions. This can be demonstrated quantitatively by examining the ratio

$$R = \frac{\sigma^{02}_{q,q+1}}{\sigma^{01}_{q,q+1}} . \qquad (23)$$

These values (with absolute errors) are listed in Table 4 for each energy and charge state and shown in Figure 13 in which it is seen that R increases with decreasing energy.

Figure 13 also indicates that R increases with charge state at a given energy, particularly the lower energies, R is noticeably greater for O^{7+} than for O^{6+} at 0.75 and 1.0 MeV/u. A reason for this could be that smal-

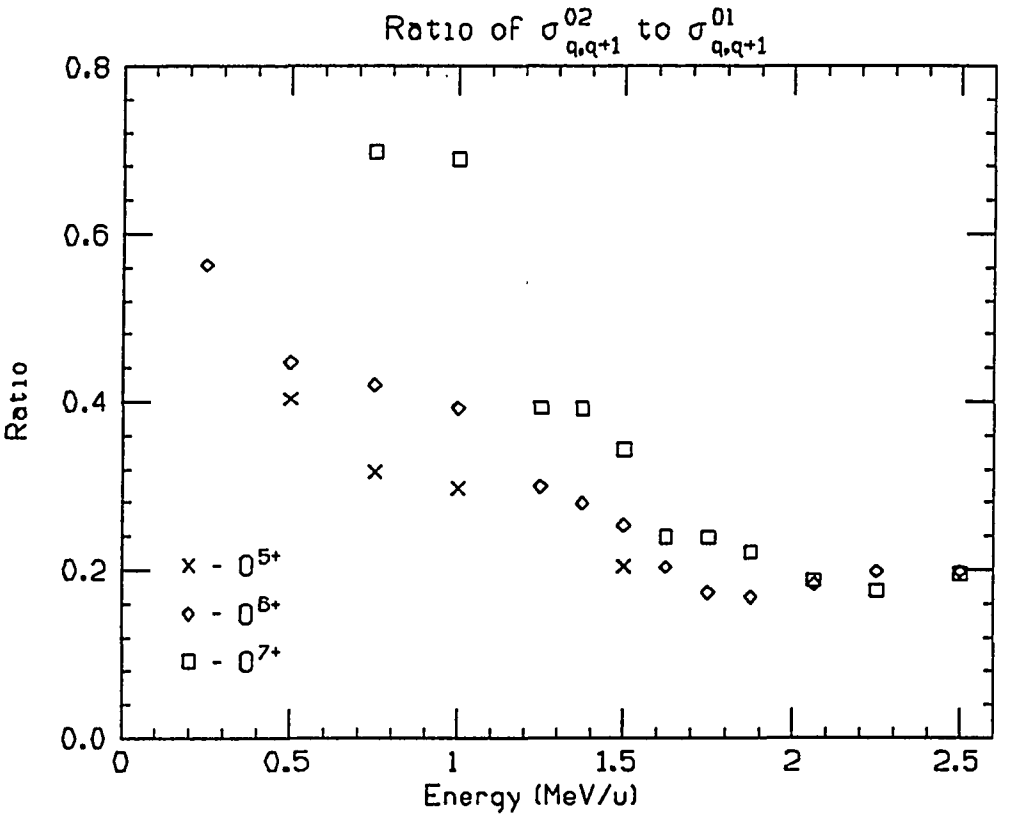

Figure 13. Ratios of Projectile Electron Loss in Coincidence With Double Ionization of the Target Atom to Projectile Electron Loss in Coincidence With Single Ionization of the Target Atom.

Table 4

Ratios of Double to Single Ionization of the Helium Target Atom Coincident With Projectile Electron Loss

q	E (MeV/u)	R	q	E (MeV/u)	R
5	0.50	0.40 +/- 0.03	6	2.07	0.18 +/- 0.03
5	0.75	0.32 +/- 0.02	6	2.25	0.20 +/- 0.03
5	1.00	0.30 +/- 0.02	6	2.50	0.20 +/- 0.02
5	1.50	0.20 +/- 0.02			
			7	0.75	0.70 +/- 0.14
6	0.25	0.56 +/- 0.06	7	1.00	0.69 +/- 0.15
6	0.50	0.45 +/- 0.06	7	1.25	0.39 +/- 0.10
6	0.75	0.42 +/- 0.06	7	1.38	0.39 +/- 0.07
6	1.00	0.40 +/- 0.04	7	1.50	0.34 +/- 0.07
6	1.25	0.30 +/- 0.04	7	1.63	0.24 +/- 0.06
6	1.38	0.28 +/- 0.03	7	1.75	0.24 +/- 0.06
6	1.50	0.25 +/- 0.03	7	1.88	0.22 +/- 0.05
6	1.63	0.20 +/- 0.03	7	2.07	0.19 +/- 0.04
6	1.75	0.17 +/- 0.03	7	2.25	0.18 +/- 0.05
6	1.88	0.17 +/- 0.03	7	2.50	0.20 +/- 0.05

ler impact parameters are required to ionize the O^{7+} projectile at these lower energies. This could then increase the probability for ionizing the He target atom and the relative number of double ionization events.

Knudsen, et al. (1984) have investigated single and double ionization of a helium target in fast collisions and have developed a relation which scales R according to charge and energy as

$$R = 2.2 \times 10^{-3} + 4.55 \times 10^{-3} \frac{q^2}{E \ln(13.123E^{0.5})}. \qquad (24)$$

This relation, which describes the ratio of double- to single-ionization of a helium target over all impact parameters, is shown as the straight line in Figure 14.

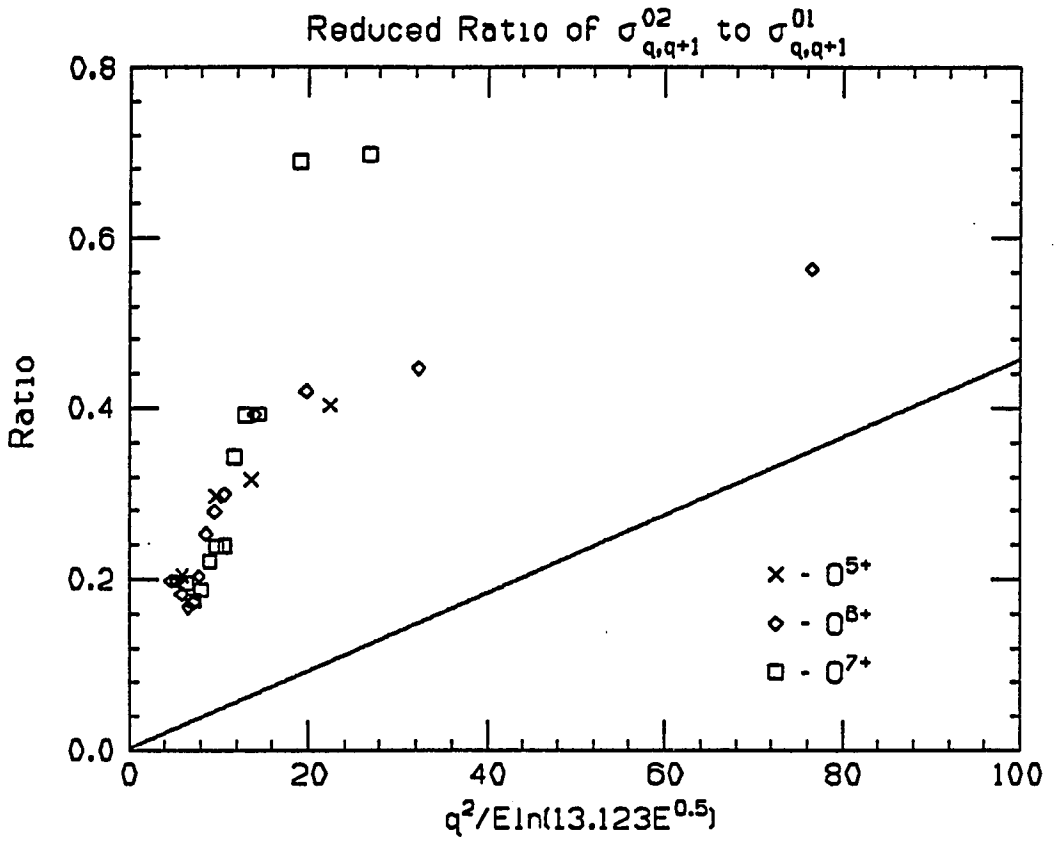

Figure 14. Ratios as a Function of $q^2/E\ln(13.123E^{0.5})$. The solid line represents the scaling relation of equation (24).

The present data, in which the oxygen projectile is simultaneously ionized along with the target (thereby limiting consideration of helium target ionization to small impact parameters only), are also shown in Figure 14. It is seen from the figure that the ratio of double- to single-target ionization coincident with simultaneous projectile electron loss is generally much greater, approximately four to five times as great, than in the work of Knudsen, et al. (1984) in which the final charge state of the projectile was not considered.

The increase in R over previous studies might be explained simply in terms of the larger probability for ionization (thereby leading to an increase in double ionization) of the target atom for the smaller impact parameter collisions which are considered when simultaneous projectile loss also occurs. It may also be that electron correlation plays a significant role in the removal of both target electrons. At present, there are no theoretical calculations with which to compare these simultaneous projectile and target ionization measurements for the O^{q+} + He collisions, so it is not possible to further assess the origin of this double target ionization mechanism.

CHAPTER V

CONCLUSION

New measurements have been presented for collisions involving highly charged oxygen (q=5,6,7,8+) incident on helium at energies of 0.25 to 2.5 MeV/u, in which the projectile ion captures or loses an electron while the target atom loses one or more electrons.

In the case of target ionization accompanied by electron capture, the current investigation of the contribution of transfer ionization to total single-electron capture, in conjunction with previously published measurements, suggests a maximum in the TI contribution for E $(keV/u)/q^{0.5} \approx 100$, in quantitative agreement with classical theory. This maximum may indicate a transition between different mechanisms being responsible for the TI process. TI fractions at energies greater than about 100 $(keV/u)/q^{0.5}$ appear to follow a $(Z/v)^2$ scaling as proposed by McGuire, Salzborn, and Muller (1987), while for the highest energies investigated, the approach to a limiting TI fraction (derived from photoionization data) suggested by these authors is not observed. The large fractions measured in this work indicate that the transfer-ionization process is responsible for a significant percentage of the total single-electron-capture cross sections

even at high velocities.

Measurements were also presented for loss of an electron from the projectile ion in coincidence with loss of one or more electrons from the target atom. Ratios of the cross sections for double ionization of the target to single ionization of the target are larger (about 4-5 times as large) when the projectile ion is also ionized than when the final projectile charge is not considered. Comparisons between the present data and previous results show that the smaller impact parameters required for ionization of the oxygen projectile appear to significantly increase the probability for doubly ionizing the helium target. The contribution of electron correlation, if any, to these simultaneous projectile and target ionization events is not presently known. Theoretical studies which may help explain these processes have yet to be conducted.

BIBLIOGRAPHY

Andersen, L. H.,Frost, M., Hvelplund, P., and Knudsen, H. (1984). Correlated two-electron effects in highly charged ion-atom collisions: Transfer ionization and transfer excitation in 20-MeV Au^{15+} + He collisions. Physical Review A, 52, 518.

Betz. H. D. (1972). Charge states and charge-changing cross sections of fast heavy ions penetrating through gaseous and solid media. Reviews of Modern Physics, 44, 465.

Choi, B. H., Merzbacher, E., and Khandelwal, G. (1973). Tables for born approximation calculations of L-subshell ionization by simple heavy charged particles. Atomic Data, 5, 291.

Cocke, C. L., DuBois, R., Grey, T. J., Justiniano, E., and Can, C. (1981). Coincidence measurements of electron capture and ionization in low-energy Ar^{q+} + (He, Ne, Ar, Xe) collisions. Physical Review Letters, 46, 1671.

Damsgaard, H., Haugen, H. K., Hvelplund, P., and Knudsen, H. (1983). Coincidence measurements of electron capture and target ionization in multiply charged Au^{q+} + (He,Ne) collisions. Physical Review A, 27, 112.

Datz, S., Hippler, R., Andersen, L. H., Dittner, P. F., Knudsen, H., Krause, H. F., Miller, P. D., Pepmiller, P. L., Rosseel, T., Stolterfoht, N., and Yamazaki, Y. (1987). Electron transfer processes in collisions of highly charged energetic (0.1 to 1.0 MeV/nucleon) ions with helium atoms. Nuclear Instruments and Methods in Physics Research, A262, 62.

Dillingham, T. R., Macdonald, J. R., and Richard, P. (1981). Ionization of one-electron ions and capture by bare and one-electron ions of C, N, O, and F on He. Physical Review A, 24, 1237.

Drawin, H. W. (1980). Atomic and molecular structure and collision data with application to fusion research. In Invited lectures and progress reports of SPIG-78, Dubrovnik, Yugoslavia, 28 Aug-2 Sep 1978 (pp. 633-659). Beograd, Yugloslavia: Institute of Physics.

DuBois, R. D. (1986). Ionization and charge transfer in He^{2+} - rare-gas collisions. Physical Review A, 33, 1595.

DuBois, R. D., and Manson, S. T. (1986). Coincidence study of doubly differential cross sections: Projectile ionization in He^{+} -He collisions. Physical Review Letters, 57, 1130.

Groh, W., Mller, A., Schlachter, A. S., and Salzborn, E. (1983). Transfer ionisation in slow collisions of multiply-charged ions with atoms. Journal of Physics B, 16, 1997.

Hansteen, J. M., and Mosebekk, O. P. (1972). Simultaneous coulomb ejection of K- and L-shell electrons by heavy charged projectiles. Physical Review Letters, 29, 1361.

Horsdal-Pedersen, E., and Larsen, L. (1979). Simultaneous ionisation of both collision partners in single collisions between H projectiles and He and Xe targets. Journal of Physics B, 12, 4099.

Hvelplund, P., Haugen, H. K., and Knudsen, H. (1981). Charge transfer and ionization in collisions between multiply charged ions and hydrogen and helium atoms. Physica Scripta, 23, 192.

Janev, R. K., and Hvelplund, P. (1981). On the cross-section scaling laws for charge exchange, ionization, and electron loss in atom-highly-charged-ion collisions. Comments on Atomic and Molecular Physics, 11, 75.

Knudsen, H., Andersen, L. H., Hvelplund, P., Astner, G., Cederquist, H., Danared, H., Liljeby, L., and Rensfelt, K. G. (1984). An experimental investigation of double ionisation of helium atoms in collisions with fast, fully stripped ions. Journal of Physics B, 17, 3545.

Knudsen, H., Haugen, H. K., and Hvelplund P. (1981). Single-electron-capture cross section for medium- and high-velocity, highly charged ions colliding with atoms. Physical Review A, 23, 597.

MacDonald, J. R., and Martin F. W. (1971). Experimental electron-transfer cross sections for collisions of oxygen ions in argon, nitrogen, and helium at energies of 7-40 MeV. Physical Review A, 4, 1965.

McGuire, J. H., Salzborn, E., and Muller, A. (1987). Simultaneous capture and ionization in helium. Physical Review A, 35, 3265.

Niehaus, A. (1980). Transfer ionization. Comments on Atomic and Molecular Physics, 9, 153.

Olson, R. E., Wetmore, A. E., and McKenzie, M. L. (1986). Double electron transitions in collisions between multiply charged ions and helium atoms. Journal of Physics B, 19, L629.

Phaneuf, R. A., Janev, R. K., and Pindzola, M. S, (1987). Atomic data for fusion, (pp. 2-4). Oakridge, TN: Oak Ridge National Laboratory. Vol. V.

Schlachter, A. S., Stearns, J. W., Graham, W. G., Berkner, K. H., Pyle, R. V., and Tanis, J. A. (1983). Electron capture for fast highly charged ions in gas targets: An empirical scaling rule. Physical Review A, 27, 3372.

Schlachter, A. S., Stearns, J. W., Berkner, K. H., Stockli, M. P., Graham, W. G., Bernstein, E. M., Clark, M. W., and Tanis, J. A. (1987). Electron capture for fast highly charged ions in He: An empirical scaling rule revisited. In XV international conference on the physics of electronic and atomic collisions, (pp. 505-506). Belfast, United Kingdom: International ICPEAC Organization.

Shah, M. B., and Gilbody, H. B. (1985). Single and double ionisation of helium by H^+, He^{2+}, and Li^{3+} ions. Journal of Physics B, 18, 899.

Sidorovich, V. A., Nikolaev, V. S., and McGuire, J. H. (1985). Calculation of charge-changing cross sections in collisions of H^+, He^{2+}, and Li^{3+} with He atoms. Physical Review A, 31, 2193.

Steigman, G. (1975). Charge transfer reactions in multiply charged ion-atom collisions. Astrophysical Journal, 199, 642.

Stockli, M. P., Bernstein, E. M., Clark, M. W., Tanis, J. A., Mowat, J. R., Graham, W. G., McFarland, R. H., Mueller, D. W., Berkner. K. H., Schlachter, A. S., and Stearns, J. W. (1986). Ionization of helium by 3.6 MeV/u Ar^{17+}. Division of Electron and Atomic Physics Meeting of the American Physical Society. Post deadline paper.